

Aerodynamic analysis of several insect-proof screens used in greenhouses

D. L. Valera*, A. J. Álvarez and F. D. Molina

Department of Rural Engineering, University of Almería. C/ Cañada de San Urbano, s/n. 04120 Almería. Spain

Abstract

Insect-proof screens constitute a physical means of protecting crops and their use has become widespread in recent years. There is no doubt as to their efficiency in controlling insects, but they do have a negative influence on greenhouse ventilation as they obstruct air-flow. It is therefore necessary not only to evaluate their efficiency as a means of protecting crops, but also to estimate the degree to which they obstruct airflow. To this end the present work analyses the aerodynamic characteristics of these screens, carrying out experiments with two devices which force a flow of air through them, thus providing data of the pressure drop as a function of air velocity. The analysis of these data has provided simple ratios of the permeability and the inertial factor as a single function of porosity.

Additional key words: agrotexiles, airflow resistance, climate control, ventilation.

Resumen

Análisis aerodinámico de diversas mallas anti-insectos utilizadas en invernaderos

Las mallas anti-insectos constituyen el método físico de protección de cultivos que más se ha extendido en los últimos años en los invernaderos. Su eficacia en el control de insectos es incuestionable, pero tienen una influencia negativa en la ventilación del invernadero, ya que representan un obstáculo que dificulta el paso de aire. Por tanto, además de evaluar la eficacia de las mallas como método de protección, es necesario estimar la resistencia que ofrecen al flujo de aire. Con este último objetivo, en este trabajo se realiza un estudio de las características aerodinámicas de diversas mallas de protección contra insectos. Para ello, se han realizado ensayos en dos dispositivos que fuerzan el paso de una corriente de aire a través de las mallas, obteniendo datos de la caída de presión en función de la velocidad. El análisis de estos datos ha permitido obtener relaciones simples de la permeabilidad y del factor inercial como una función única de la porosidad.

Palabras clave adicionales: agrotexiles, comportamiento aerodinámico, control climático, ventilación.

Introduction

The installation of plastic screens in greenhouse vents has become the most widespread means of keeping insects out in recent years. In some parts of the Mediterranean basin, plastic meshes were first used in order to limit damage to the crops at the edges of the greenhouse caused by strong winds, and also to prevent birds from entering. At that time these textiles had a very low thread density (6×6 or 6×9 threads cm^{-2}). Their great potential as a physical means of protecting crops was soon discovered and textiles with a greater density of threads started to appear, capable of preventing or limiting the

entrance of certain species of insect pests. Several authors have studied the efficiency of agrotexiles as a mean of controlling whitefly, aphids and viruses in different crops. Results show that agrotexiles may be beneficial during the coldest part of the year. Nevertheless, if not removed in time they can have a negative effect, provoking premature flowering and reducing weight per plant (Nebreda *et al.*, 2005). Barrier crops have been investigated by several authors (Ross and Gill, 1994; Kittas *et al.*, 2002), resulting in a wide range of divergent conclusions on their effectiveness. These can be an effective crop management strategy to protect against virus infection, but only under specific circumstances (Fereres, 2000). At present, in areas with a high density of greenhouses, where high losses can be incurred due to the activity of insects, the use of insect-proof screens is compulsory.

* Corresponding author: dvalera@ual.es
Received: 16-01-06; Accepted: 04-10-06.

All authors are members of the SEA.

The main advantage to be obtained by using protective screens is the reduction in insect populations inside the greenhouse, and therefore a lower incidence of diseases and the possibility of reducing the amount of phytosanitary treatments (Baker and Jones, 1989; Berlinger *et al.*, 1991). On the whole, it may be said that any means of physical protection which leads to a reduction in the amount of treatments with phytosanitary products will be of both financial and environmental benefit, as well as reducing the health risk to those workers applying the treatments and increasing trust in the market.

Among the most harmful species which growers wish to keep out of the greenhouse are the whiteflies (*Trialeurodes vaporariorum* Westwood and *Bemisia tabaci* Gennadius), western flower thrip (*Frankliniella occidentalis* Pergande), peach potato (*Myzus persicae* Sulzev) and cotton aphid (*Aphis gossypii*). They can cause both direct and indirect damage to greenhouse crops (Aparicio *et al.*, 1998; Bielza, 2003).

The present study is a contribution to the determination of airflow characteristics of insect-proof screens by means of permeability and inertial factor coefficients of Forchheimer's equation. Some commercial screens were tested using two experimental devices that force a flow of air through the porous mesh (one for velocities lower than 1 m s⁻¹ and the other for higher velocities). The results allow to obtain ratios between coefficients of Forchheimer's equation and porosity, which can then be used to calculate the airflow resistance of these screens.

Material and Methods

The efficiency of insect-proof screens as a physical barrier depends on the dimensions of the pores between the threads of the mesh. The screens are often named according to the number of threads per surface unit. However, the density of the threads alone does not suffice to determine the average dimension of the pores; the diameter of the fibres must be also known. With the above information it is possible to calculate the average length of the pores in the two main directions of the mesh:

$$L_{px} = \frac{1}{\rho_y} - D_h; \quad L_{py} = \frac{1}{\rho_x} - D_h \quad [1]$$

where L_{px} and L_{py} are the average length (in m) of the pores in the two main directions; D_h is the average diameter (in m) of the threads which make up the mesh; ρ_x and

ρ_y represent the number of threads per unit of length (threads m⁻¹) in each of the two main directions.

The main disadvantage of protective screens is that they reduce the surface area of the greenhouse devoted to ventilation. Installing screens on greenhouse vents impedes the air-flow, reducing the ventilation rate, and therefore affecting climatic variables. The reduction in ventilation surface is inversely related to the porosity of the mesh. The porosity α (m² m⁻²) expresses the relationship between the surface area of the pores (S_p), and that of the total mesh (S_t):

$$\alpha = \frac{S_p}{S_t} = \frac{L_{px} L_{py}}{(L_{px} + D_h)(L_{py} + D_h)} \quad [2]$$

The analysis of commercial protective screens is therefore of interest on two counts. Firstly it is important to know the efficiency of these materials as a physical barrier preventing the entrance of insects to the greenhouse; secondly there is a need to ascertain to what extent the mesh affects the ventilation, and by extension the microclimate inside the greenhouse. The present work focuses on the latter. The analysis of the efficiency of these screens as a means of protecting crops basically consists of the geometrical study of the pores and the comparison of the measurements obtained with the characteristic sizes of the most harmful pest species. Analysis of the mesh's resistance to airflow is carried out using devices which force a current of air through the porous meshes, thus allowing the measurement of the pressure loss caused by the porous material as a function of air velocity.

Several authors have studied the flow-resistance characteristics of various screening materials and tried to find their effect on greenhouse ventilation. In those studies, the resistance to airflow caused by the screens was determined either by using equations derived for free and forced fluid flow through porous materials or by means of a coefficient of discharge incorporated into Bernoulli's equation (Teitel, 2001). Miguel *et al.* (1997) studied the characteristics of several types of mesh used in greenhouses by means of experiments in a wind tunnel. The data obtained related the pressure drop due to the mesh with air velocity. This approach, since used by several authors (Dierickx, 1998; Miguel, 1998a,b; Muñoz *et al.*, 1999), is based on Forchheimer's equation, which describes the airflow through a porous medium:

$$\frac{\partial P}{\partial x} = \frac{\mu}{K} u + \rho \left(\frac{Y}{K^{1/2}} \right) |u| u \quad [3]$$

where P is the pressure (in Pa), x is the screen thickness (in m), μ is the dynamic viscosity (in Pa s); K is the permeability of the screen (in m^2); u is air velocity in (m s^{-1}); ρ is the air density (in kg m^{-3}); and Y is the inertial factor (dimensionless).

For velocities of airflow which imply Reynolds numbers over 150 (Teitel, 2001), the viscous forces do not dominate the flow, and therefore the first term of the second member of Eq. [3] can be discarded, obtaining the following Bernoulli equation:

$$\Delta P = \frac{1}{2} \rho F_m u^2 \quad [4]$$

where F_m is a pressure loss coefficient due to the presence of the screen, related to the discharge coefficient C_{dm} through the pores of the mesh as follows:

$$F_m = \frac{1}{C_{dm}^2} \quad [5]$$

In any case, as Muñoz *et al.* (1999) stated based on the empirical relationships obtained by Miguel *et al.* (1997), the values of pressure drop given by Eqs. [3] and [4] show very small differences for the wind speed interval of between 0 and 3 m s^{-1} .

There are different expressions to estimate the value of the pressure loss coefficient. Brundrett (1993) proposed the following for metallic mesh:

$$F_m = \left(\frac{\sigma_{mo}}{\sigma_c} \frac{7.125}{Re} + \frac{0.88}{\log(Re + 1.25)} + 0.055 \cdot \log(Re) \right) \left(\frac{1 - \alpha^2}{\alpha^2} \right) \quad [6]$$

where σ_{mo} and σ_c are the kinetic energy and momentum correction factors and Re is the Reynolds number. Based on this equation, Bailey *et al.* (2003) obtained a similar

expression to the previous one for the specific case of insect-proof screens:

$$F_m = \left(\frac{18}{Re} + \frac{0.75}{\log(Re + 1.25)} + 0.055 \cdot \log(Re) \right) \left(\frac{1 - \alpha^2}{\alpha^2} \right) \quad [7]$$

Linker *et al.* (2002) also proposed an expression to determine the pressure loss coefficient as a function of porosity and the Reynolds number:

$$F_m = \left(\frac{13}{Re} + 0.82 \right) \left(\frac{1 - \alpha^2}{\alpha^2} \right) \quad [8]$$

Wind tunnel

The experimental devices used force a current of air through the porous mesh, allowing the resulting pressure drop to be measured as a function of air velocity. The first experiments were carried out in a 4.74 m long low-speed, open-circuit wind tunnel (Fig. 1) of circular cross-section (38.8 cm diameter). This device is able to produce an airflow of up to 10 m s^{-1} , and is divided into the following parts: flow conditioner, contraction, test section, diffuser and fan. The contraction section is the most important element of the wind tunnel (Fang, 1997). Conical in shape, its purpose is to accelerate the airflow as it advances towards the test section. Generally, the contraction area ratio is the most important factor to bear in mind, as it affects the uniformity of flow, the possibility of flow separation and downstream turbulence level (Fang *et al.*, 2001). Once the contraction ratio is determined, the nozzle shape and length also play an important role in the design, affecting the uniformity of the speed-profile and the boundary layer

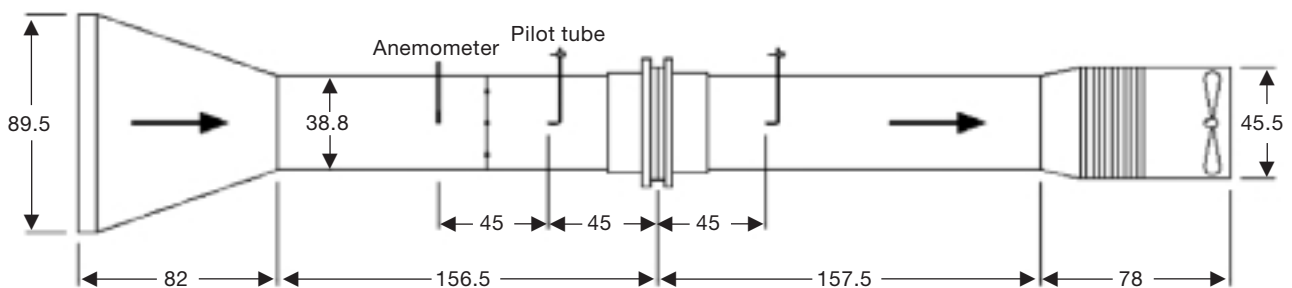


Figure 1. Diagram of the wind tunnel (all figures are in cm).

(Morel, 1975). The tunnel used in this experiment has a contraction ratio of 1:5.32 and the coefficient between the entrance diameter and the length of the contraction section is 0.92.

The airflow was propelled by an HCT-45 axial fan (Sodeca S.A., Sant Quirze de Besora, Barcelona, Spain) which can reach a velocity of 2,865 rpm and a maximum flow volume of 12,800 m³ h⁻¹. A Micromaster 420 AC Inverter was used to regulate the fan speed (Siemens España S.A., Madrid, Spain) at an output frequency of between 0 and 50 Hz and at a resolution of 0.01 Hz.

Control of air velocity in the test section of the wind tunnel was carried out according to the analogical input of the inverter. These inputs are fed by a continuous current between 0 and 10 V, and there is a linear relationship with the response of the inverter (from 0 to 50 Hz). The inputs are controlled by means of an electronic circuit incorporating a microprocessor which receives instructions from a PC. In this way the inverter can be operated remotely and automatically.

Two 4 mm diameter Pitot tubes (Airflow Developments Ltd, Buckinghamshire, England) were used to measure the static pressure. These were placed 450 mm upstream and downstream from the central axis of the assay section. The static pressure outlets of both Pitot tubes were connected to a differential pressure transducer SI 727 (Special Instruments, Nörtingen, Germany). The pressure transducer range was 200 Pa and its accuracy $\pm 0.25\%$ full scale. Hysteresis and reproducibility were $\pm 0.1\%$ full scale, and temperature error was $\pm 0.025\% \text{ K}^{-1}$, with a 0-10 V signal output.

Air velocity was measured 950 mm upstream from the test section using an EE70-VT32C5 directional hot-film anemometer (Elektronik, Engerwitzdort, Austria). This sensor has a range of between 0 and 10 m s⁻¹ and a precision of 0.1 m s⁻¹. It can also measure the temperature of the flow in a range of between 0 and 50°C and with an accuracy of $\pm 0.5^\circ\text{C}$.

Suction device

For speeds of below 1 m s⁻¹ a suction device was used to analyse the mesh (Fig. 2). This consists of a circular test duct (115 mm diameter, 220 mm length) made of transparent PVC. Twenty samples of the same mesh were placed in the test duct separated by PVC rings (10 mm thick, 115 mm external diameter and 70 mm

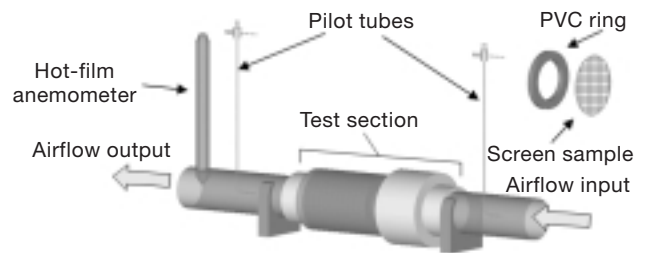


Figure 2. Suction device.

internal diameter). By testing several samples simultaneously, this device allows pressure drops to be produced which can be detected by the measurement apparatus.

Downstream from the test duct, the device was connected to a water reservoir by means of a flexible tube. The measurements were based on the pressure drop caused by natural suction of air through the samples as a result of water flow induced by gravity (Miguel *et al.*, 1997). Air velocity can be controlled by regulating the flow of water. Nevertheless, using the water reservoir this device is both complicated to assemble and difficult to regulate. As a result, an alternative was considered: the airflow through the mesh could be produced using a small NMB-4715KL fan (NMB Technologies Inc., Chatsworth, USA) directly connected downstream from the test duct. In order to vary air velocity an electronic circuit was designed which allows the direct control of the speed of a DC motor. This was achieved by cutting the power supply by means of a Pulse Width Modulation (PWM). The circuit generates a square wave with a variable on-to-off ratio, enabling the motor speed to be modified. No statistical differences were observed between tests made with the fan or the water reservoir. For the sake of simplicity, therefore, the fan was used for air supply.

In order to measure the drop in air pressure on passing through the mesh, two Pitot tubes and a pressure transducer were used, similar to those used in the wind tunnel. The Pitot tubes were placed 150 mm upstream and 90 mm downstream from the test duct. Air velocity was measured with an EE70-VT31C3 hot film anemometer (Elektronik, Engerwitzdort, Austria) with a range of between 0 and 2 m s⁻¹ and a precision of 0.05 m s⁻¹. This sensor was placed 200 mm downstream from the test duct and allowed the temperature of the flow to be measured, offering values ranging from 0 to 50°C and with an accuracy of $\pm 0.5^\circ\text{C}$.

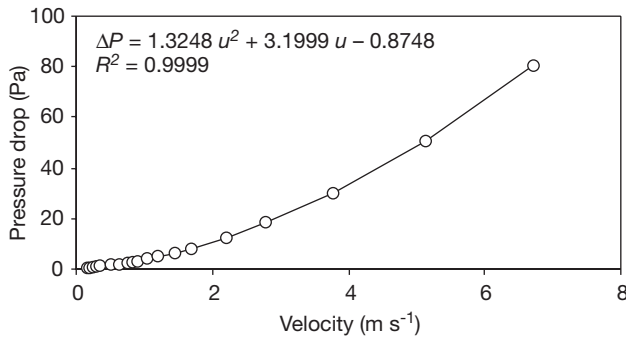


Figure 1. Pressure drop versus velocity (mesh 7).

Results and Discussion

Eleven different types of mesh have been tested. The experimental designs described above allowed pairs of data to be obtained relating the pressure drop caused by the mesh and the approach speed of the airflow. At speeds below 1 m s^{-1} the values were measured with the suction device, whereas at higher speeds measurements were recorded in the wind tunnel. Fig. 3 shows pressure drop versus air velocity. Good agreement was found, with high coefficient of determination (R^2).

It can be observed that the best fit equation of the relationship between the two variables is a second order polynomial:

$$\Delta P = a u^2 + b u + c \quad [9]$$

Equating the first and second-order terms, respectively, of the experimental polynomial [Eq. 9] and Forchheimer's equation [Eq. 3], the following expressions are obtained, allowing the permeability value K and the inertial factor Y to be determined. The presence of the free term in the fits [Eq. 9] and its nega-

tive sign are due to the tendency of the curve between the maximum airflow velocity in the assays and the minimum measurable velocity threshold, which is conditioned by the accuracy of the anemometer. The value of the free term is neglected.

$$K = \frac{\Delta x \mu}{b}, \quad Y = \frac{a \sqrt{K}}{\Delta x \rho} \quad [10]$$

where Δx is the thickness of the mesh (in m). The values of Δx and the remaining geometrical parameters were obtained using the Euclides v.1.4 software designed for this purpose (Department of Rural Engineering, University of Almería, Spain). Table 1 summarises the geometrical characterisation analyses.

Once the thickness of the mesh (Δx) was known, as well as coefficients a and b of the first and second order terms in Eq. [9], and bearing in mind the density ρ and dynamic air viscosity μ for the experimental conditions, the permeability and inertial factor could be calculated for the 11 types of mesh assayed (Table 2).

As Table 2 shows, permeability values tend to increase as the porosity of the mesh increases. The inertial factor, on the other hand, tends to decrease as porosity increases. If the geometric characteristics of the mesh are accepted to have a very slight influence on values K and Y (Miguel *et al.*, 1997), both parameters can be obtained as a function of porosity.

Figs. 4 and 5 show the permeability and inertial factor of the mesh versus porosity. The best fit equations for the experimental data are as follows:

$$K = -1.81 \cdot 10^{-8} \alpha^2 + 2.22 \cdot 10^{-8} \alpha - 4.47 \cdot 10^{-9} \quad [11]$$

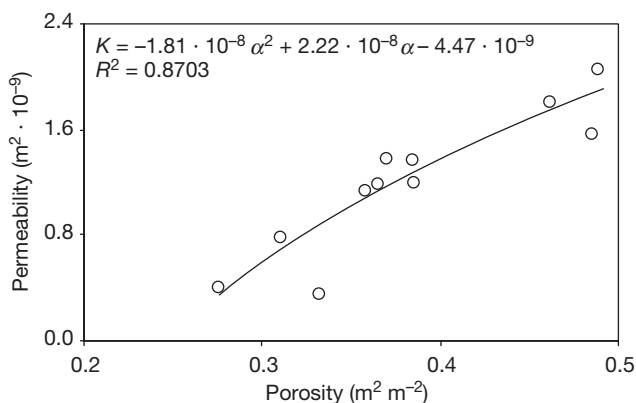
$$Y = \frac{5.96 \cdot 10^{-2}}{\alpha^{1.18}} \quad [12]$$

Table 1. Geometrical characteristics of the 11 meshes analysed

| Sample | $\rho_x \times \rho_y$ (fibre cm^2) | L_{px} (μm) | L_{py} (μm) | D_h (μm) | α ($\text{m}^2 \text{m}^{-2}$) | Δx (μm) |
|--------|--|----------------------------|----------------------------|-------------------------|---|------------------------------|
| 1 | 18.6 × 9.4 | 267.8 ± 35.6 | 795.3 ± 28.9 | 271.0 | 0.371 | 438.6 |
| 2 | 10.0 × 14.6 | 748.8 ± 23.6 | 415.6 ± 25.9 | 260.7 | 0.458 | 357.5 |
| 3 | 19.4 × 9.2 | 256.6 ± 23.3 | 840.0 ± 20.4 | 251.2 | 0.387 | 403.2 |
| 4 | 22.2 × 10.4 | 194.9 ± 17.6 | 711.7 ± 29.7 | 251.8 | 0.319 | 438.2 |
| 5 | 19.6 × 9.5 | 245.5 ± 21.1 | 804.9 ± 20.1 | 258.4 | 0.367 | 459.1 |
| 6 | 33.2 × 17.8 | 127.2 ± 19.7 | 386.2 ± 11.1 | 175.3 | 0.288 | 284.3 |
| 7 | 9.3 × 16.3 | 771.5 ± 78.8 | 379.1 ± 56.4 | 244.7 | 0.477 | 444.0 |
| 8 | 30.7 × 19.8 | 162.6 ± 21.8 | 334.6 ± 33.9 | 165.45 | 0.336 | 281.2 |
| 9 | 20.1 × 9.7 | 247.3 ± 38.1 | 777.4 ± 40.2 | 253.2 | 0.375 | 379.9 |
| 10 | 9.5 × 15.4 | 789.7 ± 87.2 | 410.0 ± 63.0 | 253.5 | 0.483 | 453.6 |
| 11 | 9.7 × 19.6 | 775.0 ± 81.5 | 263.7 ± 60.9 | 252.6 | 0.389 | 350.9 |

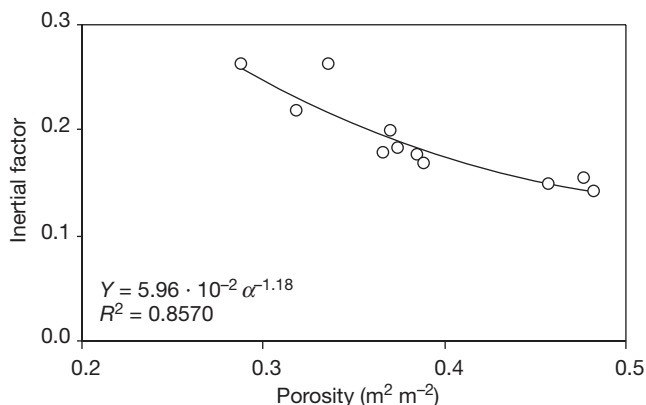
Table 2. Coefficients a , b and c for the best fit equation ($\Delta P = au^2 + bu + C$), coefficient of determination R^2 , permeability K and inertial factor Y calculated for the 11 types of mesh analysed

| Sample | a | b | c | R^2 | K (m ²) | Y |
|--------|--------|---------|---------|--------|-----------------------|-------|
| 1 | 1.9636 | 4.2360 | -1.0036 | 0.9994 | $1.29 \cdot 10^{-9}$ | 0.197 |
| 2 | 1.2046 | 2.8275 | -0.9309 | 0.9999 | $1.94 \cdot 10^{-9}$ | 0.148 |
| 3 | 1.7227 | 4.1327 | -1.0665 | 0.9999 | $1.33 \cdot 10^{-9}$ | 0.175 |
| 4 | 2.6209 | 6.2131 | -1.3334 | 0.9996 | $8.83 \cdot 10^{-10}$ | 0.218 |
| 5 | 1.7894 | 4.3186 | -1.3215 | 0.9999 | $1.27 \cdot 10^{-9}$ | 0.178 |
| 6 | 4.2335 | 11.244 | -0.9329 | 0.9993 | $4.88 \cdot 10^{-10}$ | 0.261 |
| 7 | 1.3248 | 3.1999 | -0.8748 | 0.9999 | $1.71 \cdot 10^{-9}$ | 0.153 |
| 8 | 4.2369 | 11.2333 | -0.9282 | 0.9993 | $4.88 \cdot 10^{-10}$ | 0.262 |
| 9 | 1.6887 | 3.6572 | -0.2152 | 0.9997 | $1.50 \cdot 10^{-9}$ | 0.183 |
| 10 | 1.0846 | 2.5024 | -0.6146 | 0.9999 | $2.19 \cdot 10^{-9}$ | 0.142 |
| 11 | 1.5667 | 3.7268 | -0.2735 | 0.9990 | $1.47 \cdot 10^{-9}$ | 0.168 |

**Figure 4.** Permeability K of the mesh versus porosity α for all the screen samples tested.

In other words, for the porosity range 0.29 to 0.48 (which includes the characteristic α values of these protective meshes) the best fit equation described by the relationship between permeability and porosity of the mesh is a second order polynomial, and in the case of the inertial factor and porosity the best fit is a potential equation.

The pressure drop-velocity data pairs fit second order polynomial functions, with coefficients of determination very close to unity, as described by Forchheimer's equation. The permeability and inertial factor of the meshes tested have been obtained based on these fits. Considering that the geometrical characteristics of the mesh have a negligible bearing on the values of these parameters, expressions of K and Y have been obtained as functions of porosity. The results obtained show that in the range of porosity assayed the best fit for the permeability/porosity ratio is a second order polynomial, whereas for the relationship between inertial factor and porosity it is a potential equation. These results

**Figure 5.** Inertial factor Y as a function of porosity α for all the screen samples tested.

do not agree with those obtained by other authors, since Miguel *et al.* (1997) found that the best fits for both parameters corresponded to potential equations valid for porosity values between 0.04 and 0.90.

Acknowledgements

This work has been partially funded by Projects C03-159 (*Junta de Andalucía*) and CIT-020600-2005-37 (*Ministerio de Educación y Ciencia*).

References

- APARICIO V., BELDA J.E., CASADO E., GARCÍA M., GÓMEZ V., LASTRES J., MIRASOL E., ROLDAN E., SÁEZ E., SÁNCHEZ A., TORRES M., 1998. Plagas y enfermedades en cultivos hortícolas de la provincia de Almería: control racional. Consejería de Agricultura y Pesca, Junta de Andalucía, Sevilla, Spain. 356 pp. [In Spanish].

- BAILEY B.J., MONTERO J.I., PÉREZ J., ROBERTSON A.P., BAEZA E., KAMARUDDIN R., 2003. Airflow resistance of greenhouse ventilators with and without insect screens. *Biosyst Eng* 87, 355-366.
- BAKER J.R., JONES R.K., 1989. Screening as part of insect and disease management in the greenhouse. *NC Flower Grower's Bull* 34, 1-9.
- BERLINGER M.J., MORDECHL S., LEEPER A., 1991. Application of screens to prevent whitefly penetration into greenhouses in the Mediterranean basin. *Proc Working Group Integrated Control in Protecting Crops under Mediterranean Climate*. Alassio, Italy. pp. 105-110.
- BIELZA P., 2003. Orden Thysanoptera. In: *Entomología agroforestal* (De Liñán C., ed). Ed Agrotécnicas, Madrid, Spain. pp. 603-689. [In Spanish].
- BRUNDRETT E., 1993. Prediction of pressure drop for incompressible flow through screens. *J Fluids Eng* 115, 293-242.
- DIERICKX I.E., 1998. Flow reduction of synthetic screens obtained with both a water and airflow apparatus. *J Agr Eng Res* 71, 67-73.
- FANG F.M., 1997. A design method for contractions with square end sections. *ASME J Fluids Eng* 119, 454-458.
- FANG F.M., CHEN J.C., HONG Y.T., 2001. Experimental and analytical evaluation of flow in a square-to-square wind tunnel contraction. *J Wind Eng Ind Aerodyn* 89, 247-262.
- FERERES A., 2000. Barrier crops as a cultural control measure of non-persistently transmitted aphid-borne viruses. *Virus Res* 71, 221-231.
- KITTAS C., BOULARD T., BARTZANAS T., KATSOU-LAS N., MERMIER M., 2002. Influence of an insect screen on greenhouse ventilation. *T ASAE* 45, 1083-1090.
- LINKER R., TARNOPOLSKY M., SEGNER I., 2002. Increased resistance to flow and temperature-rise resulting from dust accumulation on greenhouse insect-proof screens. *ASAE Annual International Meeting, CIGR XVth World Congress*, Chicago, USA. Paper Number: 024040, 9 pp.
- MIGUEL A.F., 1998a. Transport phenomena through porous screens and openings: from theory to greenhouse practice. *Doctoral Thesis*. Agricultural University of Wageningen, Holland. 239 pp.
- MIGUEL A.F., 1998b. Airflow through porous screens: from theory to practical considerations. *Energ Build* 28, 63-69.
- MIGUEL A.F., VAN DE BRAAK N.J., BOT G.P.A., 1997. Analysis of the airflow characteristics of greenhouse screening materials. *J Agr Eng Res* 67, 105-112.
- MOREL T., 1975. Comprehensive design of axisymmetric wind tunnel contractions. *ASME J Fluids Eng* 97, 225-233.
- MUÑOZ P., MONTERO J.I., ANTÓN A., GIUFFRIDA F., 1999. Effect of insect-proof screens and roof openings on greenhouse ventilation. *J Agr Eng Res* 73, 171-178.
- NEBRED A M., MORENO A., DÍAZ B., FERERES A., 2005. Impacto de cubiertas agrotexiles en el control de pulgones, mosca blanca y virus en cultivos de lechuga y brócoli. *Phytoma* 166, 16-26. [In Spanish].
- ROSS D.S., GILL S.A., 1994. *Insect screening for greenhouses*. Information Facts, University of Maryland at College Park, 186. 21 pp.
- TEITEL M., 2001. The effect of insect-proof screens in roof openings on greenhouse microclimate. *Agr Forest Meteorol* 110, 13-25.